DISTANCE AND REDDENING OF THE ENIGMATIC GAMMA-RAY-DETECTED NOVA V1324 SCO

Thomas Finzell[1], Laura Chomiuk[1], Ulisse Munari[2], and Frederick M. Walter[3]
[1] Department of Physics and Astronomy, Michigan State Univeristy, 567 Wilson Road, East Lansing, MI 48824-2320, USA
[2] INAF Astronomical Observatory of Padova, I-36012 Asiago (VI), Italy
[3] Department of Physics and Astronomy, Stony Brook University, Stony Brook, NY 11794-3800, USA

ABSTRACT

It has recently been discovered that some, if not all, classical novae emit GeV gamma-rays during outburst. Despite using an unreliable method to determine its distance, previous work showed that nova V1324 Sco was the most gamma-ray luminous of all gamma-ray-detected novae. We present here a different, more robust, method to determine the reddening and distance to V1324 Sco using high-resolution optical spectroscopy. Using two independent methods, we derived a reddening of $E(B-V) = 1.16 \pm 0.12$ and a distance limit of $r_D > 6.5$ kpc. This distance is $>40\%$ greater than the value used in the gamma-ray analysis, meaning that V1324 Sco has an even higher gamma-ray luminosity than previously calculated. We also use periodic modulations in the brightness, interpreted as the orbital period, in conjunction with pre-outburst photometric limits to show that a main-sequence companion is strongly favored.

Key words: binaries: general – novae, cataclysmic variables – stars: distances – stars: individual (V1324 Sco)

1. INTRODUCTION

A classical nova is the result of a thermonuclear runaway taking place on the surface of a white dwarf and are fueled by matter accreted on to the white dwarf from a companion star. These outbursts give rise to an increase in luminosity and eject between $\sim 10^{-3}$–$10^{-7} M_\odot$ of material at velocities $\gtrsim 10^3$ km s^{-1} (Gallagher & Starrfield 1978; Prialnik 1986; Shore 2012).

Nova outbursts have also been detected in the GeV gamma-rays regime with the *Fermi Gamma-ray Space Telescope* (see e.g., Cheung et al. 2010, 2012a, 2012b; Hays et al. 2013; Cheung et al. 2015). The likely source of these gamma-ray photons is strong shocks, which can generate relativistic particles via the diffusive shock acceleration mechanism and the relativistic particles can then generate gamma-rays (Blandford & Ostriker 1978; Metzger et al. 2014). But the details of shocks and shock acceleration in novae still remains a poorly understood issue, despite the potential for insight into the nature of these high-energy events (Metzger et al. 2015).

The first nova to be detected by *Fermi* was V407 Cyg, and it received considerable attention (Abdo et al. 2010; Chomiuk et al. 2012; Nelson et al. 2012; Orlando & Drake 2012). Given that V407 Cyg has a Mira giant secondary with a strong wind (a member of the symbiotic class of systems), a model to explain the gamma-rays was proposed wherein a shock was generated as the nova ejecta interacted with the dense ambient medium surrounding the red-giant companion.

This model, however, failed to explain V1324 Sco, V959 Mon, V339 Del (Ackermann et al. 2014), V1369 Cen (Cheung et al. 2013), and Nova Sgr 2015b (Cheung et al. 2015), all of which are novae that were detected by *Fermi* but lack a detectable red-giant companion (hereafter referred to as non-symbiotic gamma-ray-detected novae which, for the sake of brevity, we will refer to as NGDN). This non-detection of a red-giant companion implies that these novae have main-sequence companions with low-density circumstellar material. We note that, while it is possible for these novae to have high density circumstellar material despite not having a red-giant companion, no evidence has yet been found for dusty circumstellar material around cataclysmic variables (Harrison et al. 2013). The primary analysis for the NGDN was presented in Ackermann et al. (2014), which did not include V1369 Cen or Nova Sgr 2015b. Therefore the discussion that follows will only focus on the three non-symbiotic gamma-ray-detected nova discussed in Ackermann et al. (2014).

While no direct explanation was proposed by Ackermann et al. (2014) to explain the gamma-ray production in V1324 Sco, V959 Mon, and V339 Del, they did suggest that these novae were similar enough to one another that they represented a homogeneous population. Their evidence for a homogeneous population was that all three had similar gamma-ray spectra and light curves and were otherwise unremarkable novae. Ackermann et al. (2014) went on to suggest that it is only the close proximity of the NGDN that made them detectable by *Fermi*, and that other novae would be detected if only they were closer. However, as we show in this paper, the NGDN are not actually homogeneous, as one of them clearly stands out from the rest.

V1324 Sco is located in one of the fields continually observed by the Microlensing Observations in Astrophysics (MOA) group, and its outburst was initially detected in 2012 May as part of their high-cadence *I*-band photometry (Wagner et al. 2012). The initial detection showed a slow monotonic rise in brightness between May 14–31, followed by a very large ($\Delta I \sim 6$ mag) increase in brightness between June 1–3 (Wagner et al. 2012). Approximately two weeks after its optical brightening (2012 June 1, which we take to be the primary nova event) it was detected by the *Fermi* collaboration as a new transient source (Cheung et al. 2012a), with gamma-ray emission lasting a further ~ 2 weeks (Ackermann et al. 2014). There are several things that make V1324 Sco unusual when compared to the other NGDN.

To begin with, V1324 Sco is the most gamma-ray luminous, being at least ~ 2 times greater than the other gamma-ray-detected novae (including V407 Cyg). The estimate for the gamma-ray luminosity, done by Ackermann et al. (2014), was based on distance estimations derived using the Maximum Magnitude Rate of Decline (MMRD) method, a technique that

has been the subject of serious critiques in recent publications (see, e.g., Kasliwal et al. 2011; Cao et al. 2012). The MMRD derived distance used in Ackermann et al. (2014) was ~4.5 kpc, derived using the relation of della Valle & Livio (1995). It should be noted that Ackermann et al. (2014) do emphasize the uncertainty associated with this value, explicitly stating that a possible dust event could compromise their determination of the rate of decline in luminosity, which would alter their derived distance (this issue is also discussed in Munari et al. 2015). In this paper we find a distance limit 40% greater than that, meaning that the gamma-ray luminosity for V1324 Sco is *even greater* than initially calculated.

Another unusual aspect of V1324 Sco is that it was never detected as an X-ray source. Along with diffuse shock acceleration, shocks also generate a tremendous amount of heat, raising the ejecta to ~keV temperatures (Metzger et al. 2014, 2015). This hot shocked gas can be observed by looking for hard X-rays (Mukai & Ishida 2001; Mukai et al. 2008). A stronger shock should generate more heat, which implies that the gamma-ray luminosity and X-ray luminosity should correlate with one another. However, despite the extreme gamma-ray luminosity of V1324 Sco, it was never detected as an X-ray source (Metzger et al. 2014).

V1324 Sco clearly stands out among the NGDN, and this paper is focused on placing better constraints on this unique nova by finding values for the reddening and a distance limit. We present the results from our analysis of both spectroscopic and near-IR photometric data of V1324 Sco to find a distance limit, reddening, and constrain the luminosity class of the companion star. In Section 2 we present the details of the data observations and reduction. In Section 3 we detail the methods used to derive a value for the reddening, and in Section 4 we provide similar details for our distance limit. In Section 5 we discuss the constraints we can place on the progenitor system and in Section 6 we conclude by deriving a new lower limit on the gamma-ray luminosity using our new distance limit.

2. OBSERVATIONS

To determine the reddening we analyzed two high-resolution spectroscopic observations of V1324 Sco; a very early time Very Large Telescope (VLT) observation, and a late time observation using the *Magellan* telescope. The VLT observation was taken from the archive,[4] with the original observations reported by Wagner et al. (2012). The *Magellan* observations were obtained by the authors.

2.1. VLT Ultraviolet and Visible Echelle Spectrograph (UVES)

Spectra were taken on 2012 June 4.1 UT (+3.1 days after main outburst) by Wagner et al. (2012) using the UVES instrument on the VLT (Dekker et al. 2000). The spectra were taken as part of the follow-up conducted by the MOA group. Copies of the data were made publicly available on the ESO archive and were obtained by the authors.

Observations were made in dichroic mode, with the blue arm centered at 4370 Å (spanning 3600–4800 Å) and the red arm centered at 7600 Å (covering 5600–9300 Å), taken using two CCDs that have a chip gap between 7550–7650 Å. The slit width was 1″00 with an average seeing of 0″8, giving a resolution of $R \approx 40,000$ for the blue arm and 40,000–50,000

for the red arm. Four 1800 s integrations were taken with 1×1 binning, with each integration having an average signal-to-noise of S/N 30 per pixel for the blue arm and S/N 110–175 per pixel for the red.

The reduction was undertaken using the standard ESO Reflex data reduction pipeline, which includes flatfield correction, bias subtraction, cosmic-ray removal, spectral extraction, and wavelength calibration using comparison spectra of a ThAr lamp (see Sacco et al. 2014 for details on the data reduction procedure). The four individual spectrum frames were combined using the IRAF routine *ndcombine*, giving a final S/N per pixel of ≈60 in the blue and S/N per pixel of ≈220–350 in the red.

2.2. Magellan MIKE

Further observations were made on 2012 July 16.1 UT (+45.1 days after main outburst) using the MIKE instrument (Bernstein et al. 2003) on the 6.5 m *Magellan* Clay telescope.

The MIKE instrument also has two arms, blue (3350–5000 Å) and red (4900–9500 Å). Two 300 s integrations were taken with a 0″7 slit, giving a final resolution of $R \approx 40,000$ in the blue and $R \approx 30,000$ in the red. CCD binning was 2×2 for all integrations, giving an average S/N per pixel of ≈30 in the blue and S/N per pixel of ≈170 in the red.

The reduction for the MIKE spectra was done using the Carnegie Python tools,[5] which provides a simple pipeline data reduction procedure. Milky flats, Quartz flats, Twilight flats, ThAr comparison lamps, and bias frames were all taken during the observation run and utilized in the data reduction pipeline.

We note that the MIKE spectrum, having ~0.5 the S/N as the UVES spectrum in the red, was not used in any of our quantitative analysis. The MIKE spectrum was used instead as a qualitative check, to make sure that the spectral features seen in the UVES spectrum were not varying in time.

3. REDDENING

3.1. Reddening Measurement from Diffuse Interstellar Bands (DIBs)

We use the equivalent width (EW) of DIBs to measure the reddening, a method that has already been used in the context of novae (see, e.g., Shore et al. 2011; Munari et al. 2012). Friedman et al. (2011) found an empirical relationship between the EW of eight strong optical DIBs and the reddening along a given sight line. In V1324 Sco, one of these eight DIB features (5487.7 Å) had very low S/N (in both VLT and MIKE spectra) and was not used, and two features (6204.5 and 6283.8 Å) were discarded due to overlapping telluric features. The remaining five DIBs were used to find a value for $E(B - V)$. All of the EW values were measured using the VLT spectrum (see Figure 1) as it had a much higher S/N in the red compared to the MIKE spectrum. The specific DIB EW values are given in Table 1, and the derived $E(B - V)$ as a function of wavelength is plotted in Figure 2. The IRAF tool *splot* to measure EW values through direct integration. By iteratively varying both the bounds of integrations and the continuum flux level we determined a spread of potential EW values for each line; from this spread we determined the uncertainty in the EW values. The primary uncertainty in determining the EW values was setting the continuum flux level. From our derived values for
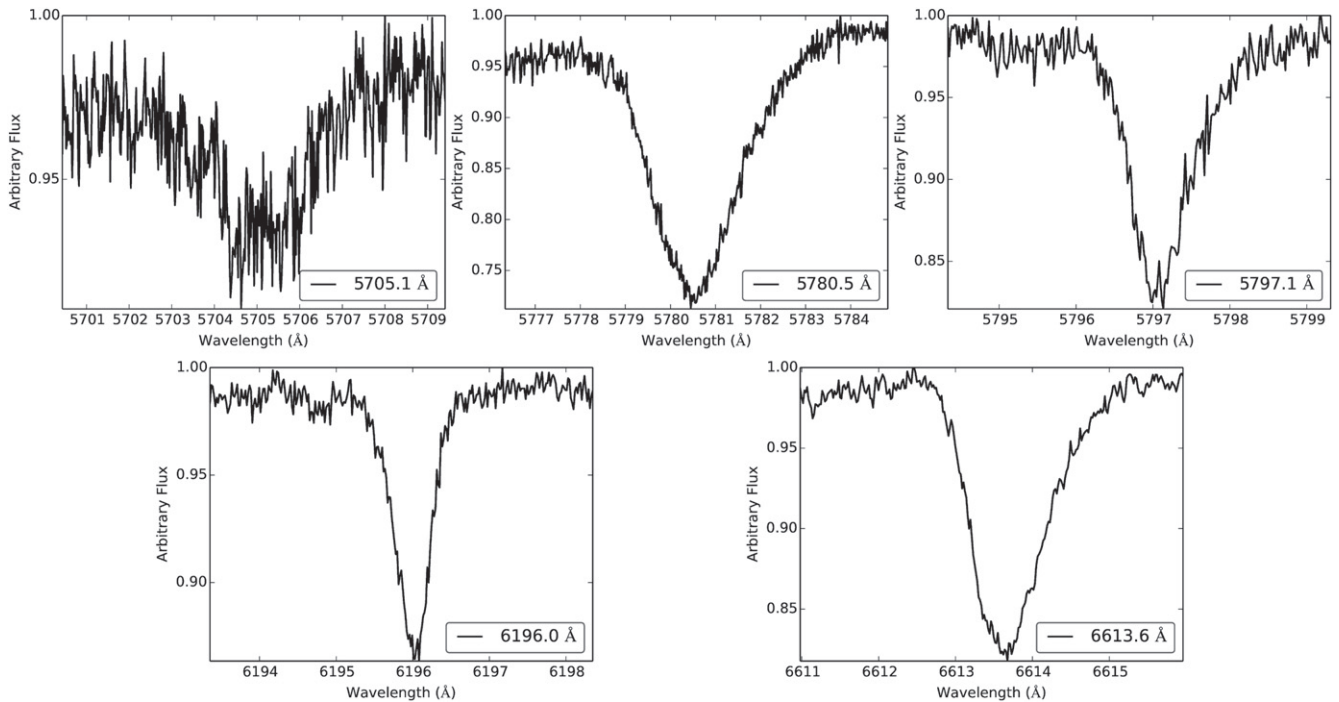

Figure 1. Five DIBs that were used to determine reddening. The largest contributor of uncertainty in the EW of the DIB features was determination of the continuum flux. This is why, in spite of the poor S/N, the 5705.1 Å feature has a comparable uncertainty to the other features.

Table 1
Best Fit Reddening Values For DIBs

DIB λ (Å)	EW (mÅ)	$E(B-V)$
5705.1	99 ± 9	1.01 ± 0.11
5780.5	581 ± 40	1.14 ± 0.08
5797.1	155 ± 16	0.86 ± 0.09
6196.0	68 ± 2	1.39 ± 0.04
6613.6	200 ± 8	0.94 ± 0.04

Figure 2. Best fit $E(B-V)$ values for all five DIBs that were analyzed (see Table 1 for the specific values). The reddening value for each DIB was determined using the best-fit values of Friedman et al. (2011). The average reddening value is $E(B-V)$ = 1.07 (the solid horizontal blue line) with an uncertainty of ±0.20 (the dashed horizontal red lines). The green band corresponds to the reddening value, $E(B-V)$ = 1.23 ± 0.15, derived using the EW of Na and K absorption features. The width of the band corresponds to the uncertainty in the derived value.

the reddening we took an error weighted average and found $E(B-V)$ = 1.07 with a 1σ uncertainty on the error weighted average of ±0.20. The uncertainty for the individual $E(B-V)$ values derived for each DIB included both the uncertainty in the fit parameters from Friedman et al. (2011) as well as the standard deviation in measured EW values. The final uncertainty in the error weighted average was dominated by the spread in derived $E(B-V)$ values for different DIB features.
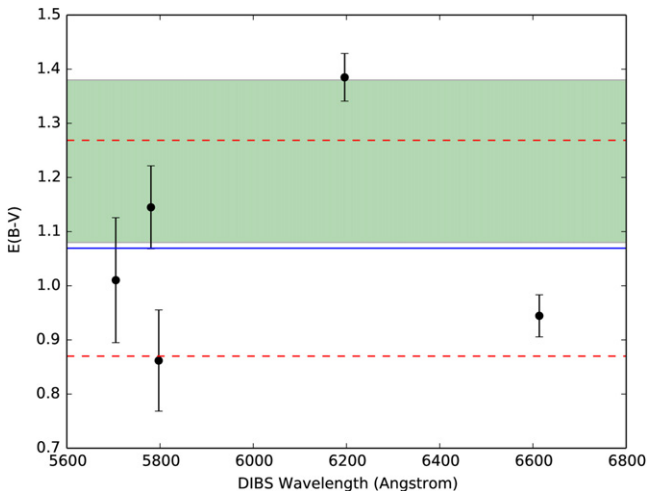
3.2. Reddening Measurement from Na and K Absorption Features

We used a second, independent, method to determine the reddening. This method utilized the empirical relationship found by Munari & Zwitter (1997), which relates reddening to the total EW of the Na I D absorption lines (at 5889.9 and 5895.9 Å) and K I absorption line (at 7698.9 Å). The material along the line of sight to an object will have some characteristic features due to interstellar absorption, and Munari & Zwitter (1997) calibrated two of these features to determine the amount of reddening each feature contributes. The sum of reddening from individual absorbing features gives the total reddening.

Munari & Zwitter (1997) found that the Na I D features are ideal for tracing reddening at low column densities, but saturates at high column densities. In these instances the K I feature, which does not saturate as easily, can be used to determine the reddening. In our case, we only needed to utilize the K I for the two Na I D features that were saturated (at -7 and $+3$ km s^{-1}).

To insure that the absorption features were the result of interstellar clouds, and not the nova itself, we compared the UVES and MIKE spectra. If the features were from the nova, we would expect them to change over time; as can be seen in the Na I D plot, which shows both the UVES and MIKE

Table 2
Reddening Values from Na I D & K I Absorption Lines

Absorption Wavelength (Å)	EW (mÅ)	$E(B-V)$	LSR Radial Velocity (km s^{-1})
5886.94	246 ± 12	0.08 ± 0.01	−136
5887.15	127 ± 6	0.04 ± 0.01	−126
5888.06	148 ± 7	0.05 ± 0.01	−79
5888.42	234 ± 12	0.08 ± 0.01	−61
5888.82	171 ± 9	0.05 ± 0.01	−41
7698.37	103 ± 5	0.39 ± 0.02	−7
7698.62	140 ± 7	0.54 ± 0.02	3
Total		1.23 ± 0.09	

spectra, the features remained constant. We did not plot the MIKE spectra for the K I features, as the S/N was very low.

Just as in the case of the DIBs features, only the UVES spectrum was used to measure the EW values as it had a higher S/N as compared to the MIKE spectrum. To avoid potential contamination of the lines with telluric features we used an archived telluric divider to remove telluric features from the UVES spectrum. Values for the EW were derived by fitting one or more Gaussian profiles to the individual spectral features. The EW, derived reddening, and velocity of the absorption features that we used to find the total reddening are given in Table 2 and Figure 3. Although the uncertainty resulting from sum of the measured quantities is ±0.09, the intrinsic scatter that Munari & Zwitter (1997) found in their calibration was 0.15 for large reddening values ($E(B-V) \geqslant 0.4$). As a result, we take 0.15 to be the uncertainty.

The reddening value found using this technique, $E(B-V) = 1.23 \pm 0.15$, is consistent (within margin of uncertainty) with the reddening derived using the DIB features.

We combine these two independent reddening measurements by taking an error weighted average of the two, which yields our final reddening value of $E(B-V) = 1.16 \pm 0.12$.

4. DISTANCE

In order to derive distance we used the reddening value found in Section 3 in conjunction with a 3D Galactic center reddening map from Schultheis et al. (2014), found using data from the *Vista Variables in the Via Lactae* (*VVV*) survey. The *VVV* survey is a ESO large program using the 4 m VISTA telescope to take near-IR photometry ($0.9-2.5\ \mu$m) of 520 square degrees toward the Milky Way Bulge to characterize variable sources. The reddening map was one of the byproducts of the exquisite *VVV* photometric dataset. The 3D map gives $E(J-K)$ reddening values as a function of: Galactic longitude (in intervals of $0°.1$), Galactic latitude (in intervals of $0°.1$), and radial distance (in intervals of 0.5 kpc, extending out to 10 kpc).

To make use of the map we needed to transform our $E(B-V)$ value into an $E(J-K)$ value given in the reddening map. To do this we found a coefficient, γ, such that $E(J-K) = \gamma E(B-V)$. The value of γ was determined using the *VVV* survey color transforms from Table 1 in Saito et al. (2012). These color transforms give the relative extinction for the *VVV* filter system in terms of $E(B-V)$, assuming a standard extinction law of Cardelli et al. (1989). From these correction values we found a γ value of 0.502, which gives

$E(J-K) = 0.58 \pm 0.06$ for our reddening value of $E(B-V) = 1.16 \pm 0.12$.

We used the average of the four points in the reddening map closest to the coordinates of V1324 Sco (R.A. = 17:50:53.90, decl. = −32:37:20.5) for our analysis. Figure 4 shows $E(J-K)$ versus radial distance r_D for the reddening map values, as well as our derived value for V1324 Sco's $E(J-K)$ reddening.

The dashed blue line in Figure 4 shows the 1σ maximum for our derived $E(J-K)$ reddening (0.62); it is clear that this value is consistent with any distance >6.5 kpc. Because of this degeneracy in $E(J-K)$ reddening we can only place a lower limit of 6.5 kpc on the distance to V1324 Sco.

5. PROGENITOR

If V1324 Sco had a giant companion like V407 Cyg then the wind from the companion could explain its exceptionally high gamma-ray luminosity. To determine if this is a feasible explanation we need to determine if the progenitor system to V1324 Sco has a giant secondary star. The strongest photometric constraints on the secondary star comes from the *VVV* Survey (Minniti et al. 2010), which obtained several epochs of near-IR photometry on the target field between 2010 July and 2011 September. We searched the catalog for all stars with non-zero K-band magnitude in a $15'' \times 15''$ cutout centered on the coordinates of V1324 Sco ($N \approx 25,000$). To qualify as a star an object had to have a *pStar* value >0.9 (see *VVV* documentation for a description of the *pStar* variable). From this sample we found that 99% of the sources had $m_K < 16.626$; given that V1324 Sco was not detected by the *VVV* survey, we use this value as a limiting magnitude.

Table 1 in Saito et al. (2012) gives the filter specific extinction for the *VVV* K band as $A_K/E(B-V) = 0.364$, and we can use our derived reddening value to obtain a K-band extinction of $\sim$0.42 mag. Without a proper upper bound on the distance to V1324 Sco we cannot place an upper limit on the distance modulus. However we can say that, if V1324 Sco were at a distance of $\gtrsim$9.5 kpc, then the distance modulus would be $\approx$15.3, meaning that the absolute K-band limit would be bright enough for the companion to be a very faint giant ($M_K \geqslant 1.3$, corresponding to a spectral type G5 giant Covey et al. 2007). However, if V1324 Sco is at the galactic center ($\sim$8.5 kpc), then it must have a dwarf companion.

While this limit is not stringent enough to rule out a giant companion, by analyzing the period of V1324 Sco we show that the a main sequence companion is strongly favored.

5.1. Constraints from the Orbital Period

Darnley et al. (2012) created a classification system for novae according to their orbital period which is a proxy for luminosity class of the secondary star. We utilize this classification scheme to help constrain the companion to V1324 Sco.

Measurements of the binary orbital period were found in the original photometry from the MOA group, who detected periodic modulations in the brightness of V1324 Sco (Wagner et al. 2012). These modulations were on the order of $\sim$0.1 mag, with a period of $\sim$1.6 hr. However, it is possible that there ellipsodial variations in the photometric light curve, which would give a secondary minimum and maximum. As a result, we consider both 1.6 and 3.2 hr for the period in our analysis.
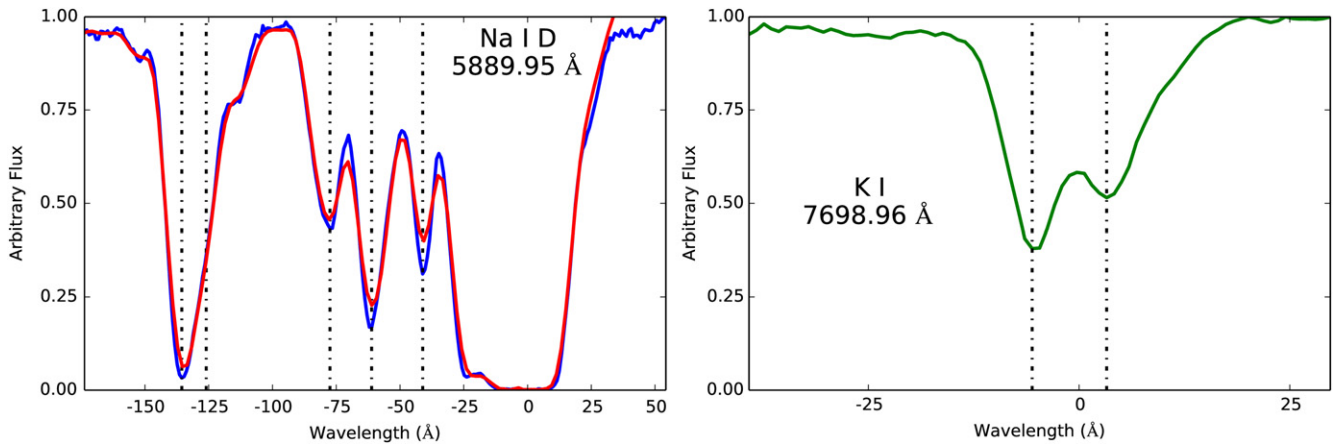
Figure 3. Sodium D (5889.95 Å) and potassium (7698.96 Å) interstellar absorption features that were used to derive a value for the reddening. The specific absorption components from Table 2 are marked as black dashed lines. We plot both the UVES and *Magellan* spectra for the sodium to show that these features are unchanging in time, meaning they are interstellar and not associated with the nova. Note that we only use the potassium absorption feature to calculate reddening when the sodium feature is saturated, which is why we are only showing the potassium in the region where the sodium is saturated.
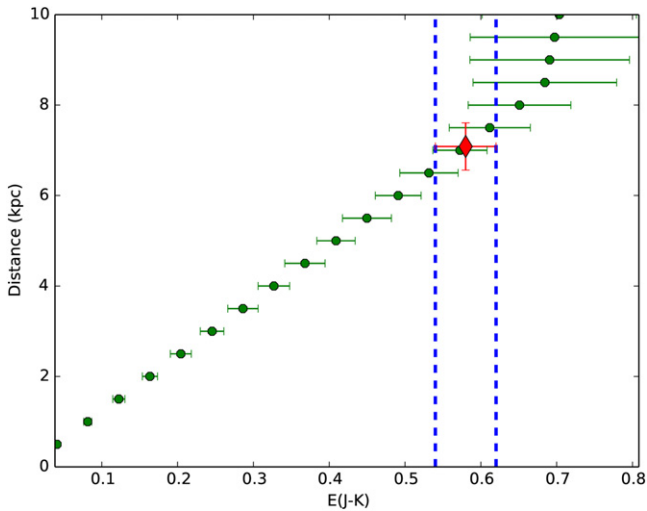
Figure 4. Green data points give the (average) $E(J - K)$ reddening values as a function of distance at the position of V1324 Sco, taken from the 3D reddening map of Schultheis et al. (2014). The red diamond indicates the derived reddening. The blue dashed lines show the 1σ extent of the derived reddening; it is clear that this value is consistent with all reddening values past 6.5 kpc.

Interestingly, if the period is 1.6 hr, V1324 Sco would be below the period gap, meaning that the angular momentum loss is driven by gravitational radiation (Knigge 2011). Only a handful of novae fall below the period gap (Wagner et al. 2012), and it has been postulated that these systems may have a different type of mass transfer mechanism that takes place in this period range (Uthas et al. 2010).

Using the value for the period within the framework of Darnley et al. (2012) (Figure 5) we see that V1324 Sco (the purple dashed line) most likely falls into the region of blue points, indicting that it has a main sequence companion.

6. CONCLUSIONS

Here we present results of the analysis of optical spectroscopy and near-IR photometry of the nova V1324 Sco to determine the reddening and a limit on the distance. We derived a reddening value using two independent methods and found $E(B - V) = 1.16 \pm 0.12$. Using this reddening value
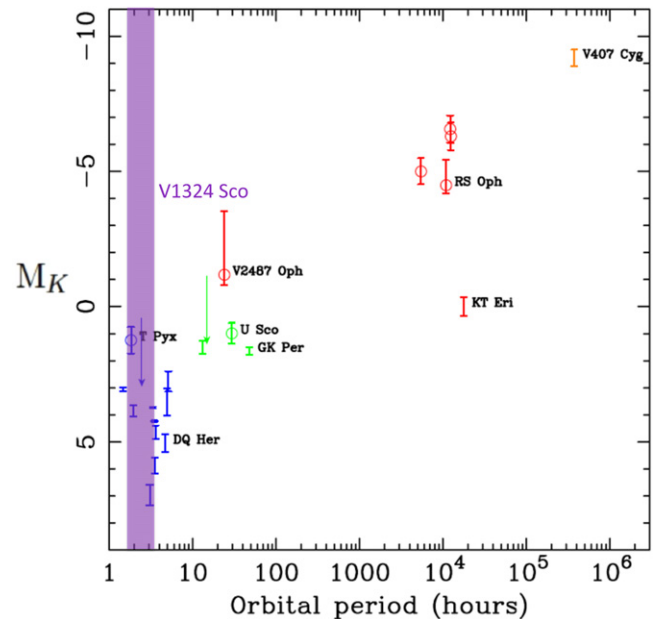

Figure 5. Plot showing the distribution of novae as a function of absolute K-band magnitude and binary orbital period, taken from Darnley et al. (2012). V1324 Sco is marked as the purple transparent line, indicating that we know the period $\sim$1.6 hr, but we cannot place a limit on the absolute K-band magnitude. The width of the purple line corresponds to the fact that the period could either be 1.6 or 3.2 hr. The colors on the plot correspond to the luminosity class of the secondary: blue is main sequence, green is sub-giant, and red is giant.

we found a distance lower limit of $r_D > 6.5$ kpc to V1324 Sco, which stands in contrast to the 4.5 kpc value used in the analysis of Ackermann et al. (2014). We also found that, while we cannot rule out a giant companion, the short period of V1324 Sco strongly favors a main sequence companion. V1324 Sco was already the most gamma-ray luminous nova when using the values from Ackermann et al. (2014); using our new distance limit of $r_D > 6.5$ kpc, we find that the gamma-ray luminosity is at least a factor of $\sim$2.1 times greater than initially calculated by Ackermann et al. (2014). We encourage deep follow-up photometry of V1324 Sco in order to place greater constraints on the companion.

REFERENCES

Abdo, A. A., Ackermann, M., Ajello, M., et al. 2010, Sci, 329, 817
Ackermann, M., Ajello, M., Albert, A., et al. 2014, Sci, 345, 554
Bernstein, R., Shectman, S. A., Gunnels, S. M., Mochnacki, S., & Athey, A. E. 2003, Proc. SPIE, 4841, 1694
Blandford, R. D., & Ostriker, J. P. 1978, ApJL, 221, L29
Cao, Y., Kasliwal, M. M., Neill, J. D., et al. 2012, ApJ, 752, 133
Cardelli, J. A., Clayton, G. C., & Mathis, J. S. 1989, ApJ, 345, 245
Cheung, C. C., Donato, D., Wallace, E., et al. 2010, ATel, 2487, 1
Cheung, C. C., Glanzman, T., & Hill, A. B. 2012a, ATel, 4284, 1
Cheung, C. C., Hays, E., Venters, T., Donato, D., & Corbet, R. H. D. 2012b, ATel, 4224, 1
Cheung, C. C., Jean, P., & Shore, S. N. 2015, ATel, 7315, 1
Cheung, C. C., Jean, P., Shore, S. N. & Fermi Large Area Telescope Collaboration 2013, ATel, 5649, 1
Chomiuk, L., Krauss, M. I., Rupen, M. P., et al. 2012, ApJ, 761, 173
Covey, K. R., Ivezić, Ž, Schlegel, D., et al. 2007, AJ, 134, 2398
Darnley, M. J., Ribeiro, V. A. R. M., Bode, M. F., Hounsell, R. A., & Williams, R. P. 2012, ApJ, 746, 61
Dekker, H., D'Odorico, S., Kaufer, A., Delabre, B., & Kotzlowski, H. 2000, Proc. SPIE, 4008, 534
della Valle, M., & Livio, M. 1995, ApJ, 452, 704
Friedman, S. D., York, D. G., McCall, B. J., et al. 2011, ApJ, 727, 33
Gallagher, J. S., & Starrfield, S. 1978, ARA&A, 16, 171
Harrison, T. E., Hamilton, R. T., Tappert, C., Hoffman, D. I., & Campbell, R. K. 2013, AJ, 145, 19
Hays, E., Cheung, T., & Ciprini, S. 2013, ATel, 5302, 1
Kasliwal, M. M., Cenko, S. B., Kulkarni, S. R., et al. 2011, ApJ, 735, 94
Knigge, C., Baraffe, I., & Patterson, J. 2011, ApJS, 194, 28
Metzger, B. D., Finzell, T., Vurm, I., et al. 2015, MNRAS, 450, 2739
Metzger, B. D., Hascoët, R., Vurm, I., et al. 2014, MNRAS, 442, 713
Minniti, D., Lucas, P. W., Emerson, J. P., et al. 2010, NewA, 15, 433
Mukai, K., & Ishida, M. 2001, ApJ, 551, 1024
Mukai, K., Orio, M., & Della Valle, M. 2008, ApJ, 677, 1248
Munari, U., Dallaporta, S., & Valisa, P. 2012, ATel, 4320, 1
Munari, U., Walter, F. M., Henden, A., et al. 2015, IBVS, 6139, 1
Munari, U., & Zwitter, T. 1997, A&A, 318, 269
Nelson, T., Donato, D., Mukai, K., Sokoloski, J., & Chomiuk, L. 2012, ApJ, 748, 43
Orlando, S., & Drake, J. J. 2012, MNRAS, 419, 2329
Prialnik, D. 1986, ApJ, 310, 222
Sacco, G. G., Morbidelli, L., Franciosini, E., et al. 2014, A&A,, 565, A113
Saito, R. K., Hempel, M., Minniti, D., et al. 2012, A&A,, 537, A107
Schultheis, M., Chen, B. Q., Jiang, B. W., et al. 2014, A&A, 566, A120
Shore, S. N. 2012, BASI, 40, 185
Shore, S. N., Augusteijn, T., Ederoclite, A., & Uthas, H. 2011, A&A, 533, L8
Uthas, H., Knigge, C., & Steeghs, D. 2010, MNRAS, 409, 237
Wagner, R. M., Dong, S., Bensby, T., et al. 2012, ATel, 4157, 1